

Article

# EEG characterization and classification based on histograms of image gradients

Rodrigo Ramele <sup>1,†</sup>, Ana Julia Villar <sup>1</sup> and Juan Miguel Santos <sup>1\*</sup>

<sup>1</sup> Computer Engineering Department, Instituto Tecnológico de Buenos Aires (ITBA); info@itba.edu.ar

\* Correspondence: rramele@itba.edu.ar; Tel.: +54-9-11-4193-9382

† Current address: C1437FBH Lavarden 315, Ciudad Autónoma de Buenos Aires, Argentina

Academic Editor: name

Version February 13, 2017 submitted to Entropy; Typeset by L<sup>A</sup>T<sub>E</sub>X using class file mdpi.cls

**Abstract:** The analysis of Electroencephalography (EEG) signals for Amyotrophic Lateral Sclerosis (ALS) patients is of ulterior importance to elucidate different patterns or markers that could improve the implementation of Brain Computer Interface (BCI). These systems are meant to provide alternative pathways to transmit volitional information which could potentially enhance patient's quality of life. Of particular interests are those which are based on the recognition of Event-Related Potentials (ERP), shown to be more robust to the unavoidable physical impairment which comes with this motor neuron disease. This work mimics what electroencephalographers have been doing clinically, visually inspecting and categorizing phenomena within the EEG, and provides a framework to analyse and characterize EEG signals, with a focus on the P300, an ERP elicited by the oddball paradigm of rare events. The validity of the method is shown by off-line processing a public dataset of ALS patients.

**Keywords:** electroencephalography (EEG); BCI; P300; ALS; classification; HOG; SIFT

## 0. Introduction

Although recent advances in neuroimaging techniques (particularly radio-nuclear and radiological scanning methods) [1] have diminished the prospects of the traditional Electroencephalography (EEG), the advent and development of digitalized devices has pressed for a revamping of this hundredth years old technology. Their versatility, ease of use, temporal resolution, ease of development and fabrication, and its proliferation as consumer devices, are pushing EEG to become the de-facto non invasive portable or ambulatory method to access and harness brain information [2]

Key contribution to this development has been the field of Brain Computer Interfaces (BCI) [3] which is the pursuit of the development of a new channel of communication particularly aimed to persons affected by neuro-degenerative diseases.

One noteworthy aspect of this novel communication channel is the ability to volitionally transmit information from the Central Nervous System (CNS) to a computer device and from there use that information to control a wheelchair [4], as input to a speller application [5], or as aiding tool in a rehabilitation procedure [6]. The holy grail of BCI is to implement a new complete and alternative pathway to restore lost locomotion [3].

EEG signals are remarkably complex and have been characterized as a multichannel non-stationary stochastic process and even considered random enough as to be used as a source of pseudo random number generator [7]. Additionally, they have high variability between different subjects and even between different moments for the same subject, requiring an adaptive and

co-adaptive calibration and learning procedures [8]. Hence, this imposes an outstanding challenge that is necessary to overcome in order to extract information from raw EEG signals.

EEG markers [8] that can be used to volitionally transmit information are limited, and each one of them has a particular set or combination of appropriate methods to decode them. Inevitably, it is often necessary to implement many distinct and specialized algorithmic methods, to filter the signal, enhance its SNR, and try to determine some meaning out of it. NEED REVIEW Patients suffering from ALS their brain signals do suffer slow and deteriorating changes that may lead to different EEG patterns alterations [9,10].

BCI has gained mainstream public awareness and recently even held a peculiar Olympics [10] and been broadcasted during the inauguration ceremony of the 2014 Soccer World Cup. New developments have overcome the out-of-the-lab high-bar and they are starting to be used in real world environments [11]. However, they still lack the necessary robustness, and its performance is well behind any other method of human computer interaction, including any kind of detection of remaining muscular movement [8].

In this work a new method to characterize EEG signals is presented, expanded and detailed. Its validity is verified by processing off-line data for ALS patients. This is the continuation of the work previously presented in [12], where it was applied to rhythmic patterns, and that it can be extended to describe transient events like those produced by the P300 [13].

The method is based on the morphological analysis of the shape of the EEG signal [14,15] and was inspired by mimicking what traditionally electroencephalographers have been performing for almost a century: visually inspecting raw signals [16].

In brief, this paper reports a straightforward method to, first characterize EEG signals based on the identification of their morphological shapes, and how this characterization can be used to implement a BCI scheme to identify Event Related Potentials of ALS patients, particularly the well-known P300, on an off-line and public dataset.

## 1. Materials and Methods

To verify the validity of the proposed framework and method, the public dataset 008-2014 [17] published on the BNCI-Horizon website [18] by IRCCS Fondazione Santa Lucia, was used to perform a binary classification task on the provided signals. The algorithm was implemented using the VLFeat [19] Computer Vision libraries on MATLAB 2014a (Mathworks Inc., Natick, MA, USA).

### 1.1. Experimental protocol

The protocol is explained in [17] but can be summarized as follows: 8 subjects with confirmed diagnoses but on different stages of ALS disease, were recruited and accepted to perform the experiments. The P300 [13] is a positive deflection of the EEG signal which occurs 300 ms after the onset of a rare and deviant stimulus that the subject is expected to attend. It is produced under the oddball paradigm [3] and though it is quite consistent across different subjects, it is small ( $\pm 5\mu V$ ) compared to the ongoing EEG activity. The P300 detection task designed for this experiment was meant to spell 7 words of 5 letter each, using the traditional P300 Speller Matrix, where the flashings of rows and columns provide the deviant stimulus required to elicit this physiological response. The first 3 runs were used for training and the remaining 4 for testing with visual feedback. A trial, for this experiment, was defined as every attempt to select a letter from the speller, and it was composed of signal segments corresponding to 10 repetitions of flashes of 6 rows and 6 columns of the traditional 6x6 P300 matrix, yielding 120 repetitions. Flashing of row/columns was performed for 0.125 s, following by a resting period of the same length. After 120 repetitions an inter-trial pause was included before resuming with the following letter.

The gathered dataset was sampled at 256 Hz and consisted of an EEG matrix for electrode channels Fz,Cz,Pz,Oz,P3,P4,PO7 and PO8, identified according to the 10-20 International System, for each one of the 8 subjects.

## 1.2. Algorithm

The proposed algorithm was developed to perform a binary classification task, determining the appearance or not of the P300 response on each corresponding signal segment. If it was present, the segment was labelled as class 1, a *hit*, and its absent was identified as class 2, a *no-hit*.

### 1.2.1. Preprocessing

The mandatory first step is to enhance the SNR of the P300 pattern above the level of basal EEG. The processing pipeline starts by applying a notch filter to the raw signal, a decimation with an FIR filter of order 30 from the original 256 Hz to 32 Hz and finally applying a 4th degree 10 Hz lowpass Butterworth filter.

### 1.2.2. Segmentation, Artefact Removal and Signal Averaging

The EEG matrix is processed on a channel by channel basis. For each word, each letter, a segment of EEG signal is extracted that encompass 10 repetitions of 12 flashings, 6 rows and 6 columns. For every 12 flashing stimuli, i.e. one complete sequence of repetitions of each row/column, a basic artefact removal procedure of removing the entire segment if any signal goes above 70  $\mu\text{V}$  is applied.

From every segment of 12 flashings, two epoch were obtained when the signal was labelled as *hit* and two when the signal was labelled as a *no-hit* of 1s length both (256 sample points).

These segments, 20 for each class, are later point-to-point averaged for the whole trial. It is important to remark that only 2 out of 10 available segments marked as a *no-hit* were extracted in order to avoid generating unbalanced averaging signals (see Results section 2). This finally led to 2 averaged signals for each of the 5 letters, for the 7 words, comprising a set of 70 averaged signals [20].

### 1.2.3. Features

The central part of this method is the feature generation: the histogram of image gradients. To do so, the first step is the transformation of the signal into a temporary binary image.

The signal is first scaled and centered at zero by

$$\tilde{x}(t, c) = \lfloor \gamma \cdot (x(t, c) - \bar{x}(t, c)) \rfloor \quad (1)$$

where  $\gamma$  is the image scale,  $t$  is time and  $x(t, c)$  is the EEG matrix defined for each  $t$  and for a particular channel  $c$ .

Then the image is constructed by

$$I(z_1, z_2) = \begin{cases} 255 & z_1 = \gamma \cdot t; z_2 = \tilde{x}(t, c) + z(c) \\ 0 & \text{otherwise} \end{cases} \quad (2)$$

and used to derive local representations that will capture the visual shape of the signal.

Finally, the histogram of gradients, which is based on the SIFT [21] descriptor, a technique from Computer Vision, is calculated on local image patches centered on sample points [19]. To do this, the patch is divided in 16 blocks, arranged in a 4x4 grid and centered on  $T = (x, y)$ , a location within the image. The values of the image gradients for each angle bin are accumulated through

$$h(p, i, j) = 3 \cdot s \int w_{\text{ang}}(\angle J(\mathbf{x}) - \theta_p) w_{ij} \left( \frac{\mathbf{x} - T}{3s} \right) |J(\mathbf{x})| d\mathbf{x} \quad (3)$$

where  $s$  is the size of the local patch, which can be converted into pixels by doing  $Px = 4 \cdot 3 \cdot s$ ,  $\angle J(\mathbf{x})$  is the angle of the gradient vector  $J(\mathbf{x})$  found at each one of the 16 blocks of the patch, whereas  $\theta_p$  is one of the bin angles. On the other hand  $x = (x_i, x_j)$  corresponds to each one of the pixels of the local patch, and  $w_{\text{ang}}$  and  $w_{ij}$  are linear interpolation functions [21].

Summarizing, each block of the patch defines 8 different bins of the histogram. On each one of these bins the magnitude of the image gradients at different angles is summed up (from 0 to 360, on steps of 45 degrees). As the patch is 4x4, it gives a descriptor of 128 dimension as shown on Figure 1.

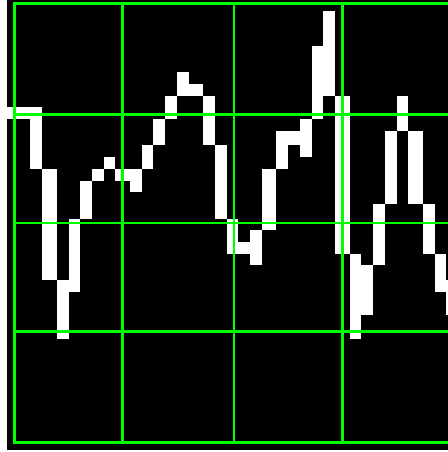


**Figure 1.** The local patch is located around a sample point plotted on the temporary image. All the sample points are interpolated using the Bresenham algorithm. The 4x4 block grid can be seen on the patch as well as the green arrows showing the dominant gradient on each block.

#### 1.2.4. Classification

The classification is carried out by using a discriminative semi-supervised classification method, the Naive Bayes Nearest Neighbour (NBNN) [22] and the first step consists in extracting labelled descriptors from the training set for each class which are thus grouped together in two KD-tree [19] database structures.

While doing classification based on local features, which encode partial information, one problem that frequently arises is how to ensemble the individual classification of each local characteristic to the image that were used to derive those descriptors.

The NBNN algorithm tackles this problem by comparing each image against a whole classification class which is characterized by the set of descriptors that are closest to each one of the descriptors obtained for the query image. The algorithm is based on 4,

$$\hat{C} = \underset{C}{\operatorname{argmin}} \sum \|d_i - NN_C(d_i)\|^2 \quad (4)$$

where the predicted class  $\hat{C}$  of a query image is calculated as the class  $C$  that minimize the summation of the  $L^2$  distance between each descriptor  $d_i$  that belongs to the query image and its corresponding near neighbour  $NN_C(d_i)$  descriptor from each class.

#### 1.2.5. Parameters

This method's parameters were selected according to the experimental protocol. As the P300 event latency varies greatly between subjects, it is necessary to provide a descriptor that will be able to capture an entire transient event. Equations 5 and 6 can be used to map the original signal parameters to local image patch structure.

$$s = \frac{\Delta\mu V}{4 \cdot 3} \cdot \gamma \quad (5)$$

$$s = \frac{\lambda \cdot Fs}{4 \cdot 3} \cdot \gamma \quad (6)$$

where  $F_s$  is the sample frequency of the EEG signal,  $\lambda$  is the length in seconds covered by the patch, and  $\mu V$  corresponds to the amplitude in microvolts that can be covered by the height of the patch. By using  $s = 3$  and a double scale of the image  $\gamma = 2$  this gives the local patch, and the descriptor, the ability to identify events of  $18 \mu V$  of amplitude of  $\lambda = 0.5s$ . Finally, descriptors locations  $T$  were selected as suggested by the dataset publisher [17] between 0.2s and 0.7s after the onset of the stimulus.

## 2. Results

In Figure 2 the grand average (point-to-point) for all the subjects using the whole trial (i.e. 120 repetitions) is shown. The P300 characteristic curve can be seen particularly in subjects 2, and 6 and in a lesser extend in the remaining subjects. In order to obtain a valid binary classification on averaged signals, particular care was observed to avoid unbalanced samples, because that may introduce a bias in the classification procedure (the variance of average signals is inversely proportional to the number of samples and the procedure would be discriminating signals with different variances). Especially in the case of the P300 response, the oddball paradigm requires that one of the stimuli need to be infrequent so that will unavoidably force the data to be unbalanced (i.e. an unequal number of trials in each condition) [23].

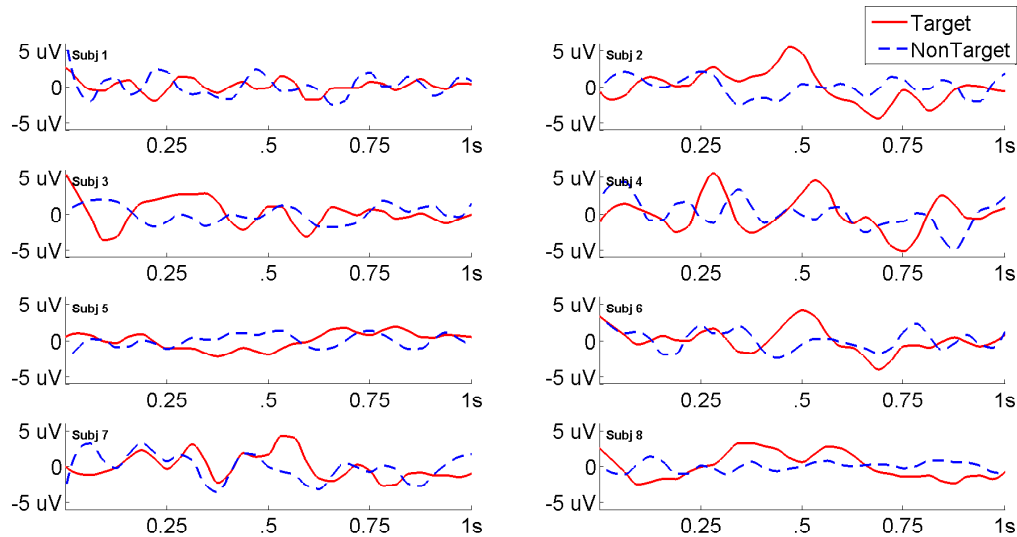


**Figure 2.** Point-To-Point grand averages of epochs obtained for hits (solid line) and no hits (dashed line) for each one of the 8 subjects for channel Cz. The P300 characteristic curve can be well identified particularly on subjects 2 and 6.

Results are shown in Table 1 where BCI accuracy for the Cz channel is calculated and compared with the values obtained by the publisher of the dataset [17]. Additionally the best performing channel is informed as well as its accuracy value. It is of particular interest that using this method, the best performing channel was not always Cz, and instead occipital channels PO8 and PO7 showed very good performance indeed [6,11].

**Table 1.** Accuracy levels obtained by a 3-fold cross validation. The values reported by the dataset publishers for Cz are reproduced here for comparison. Additionally, BCI accuracies for channel Cz can be seen as well as performance levels and their standard deviation obtained for the BPC, the best performing channel for each subject.

Participant	Original Cz	ACC at Cz	BPC	Performance
1	0.84	0.79	Cz	$0.79 \pm 0.01$
2	0.86	0.81	PO7	$0.93 \pm 0.01$
3	0.87	0.78	Cz	$0.78 \pm 0.03$
4	0.86	0.68	PO8	$0.90 \pm 0.01$
5	0.86	0.80	PO7	$0.93 \pm 0.01$
6	0.89	0.96	Cz	$0.96 \pm 0.01$
7	0.89	0.78	PO7	$0.93 \pm 0.01$
8	0.92	0.91	PO7	$1.00 \pm 0.00$

The ITR, or BTR, in the case of reactive BCIs [3] strongly depends on the amount of signal averaging required to transmit a valid and robust selection. There is a trade-off that needs to be balanced between the required number of repetitions for each trial to guarantee robust transmission and the the achieved speed of transmission affected by the repetitions. As detailed in the table 2 by applying this method, accuracy levels are only reduced in 20 percent even by using only one sequence of 12 repetitions (i.e. an entire flashing of the whole matrix).

**Table 2.** Accuracy levels obtained by performing a BCI simulation on the testing dataset (4 letters). The BPC, best performing channel is shown and also performance levels for the 120, 60 and 12 repetitions. Finally the PR, performance reduction as a rate of reduction compared to the accuracy obtained using the entire trial, is described. Almost all the subjects performed around 70% even by averaging only 2 epochs for each class.

Participant	BPC	ACC@120	ACC@60	ACC@12	PR
1	Cz	0.80	0.82	0.72	9%
2	PO7	0.93	0.78	0.75	18%
3	Cz	0.80	0.82	0.72	9%
4	PO8	0.93	0.78	0.65	29%
5	PO7	0.93	0.78	0.75	18%
6	Cz	0.80	0.82	0.72	9%
7	PO7	0.93	0.78	0.75	18%
8	PO7	0.93	0.78	0.75	18%

### 3. Discussion

This method, different from other methods which is based on the nonlinearity of the gradient of histograms which can be used to detect is also based on how the image look like. SNR of p300 and how to detect it Check if you can use this to detect any kind of transient signal. Compare if it is possible with the descriptors from one subject, discriminate the others. Channal identification based on the metric distance between the bags

### 4. Conclusion

A method to characterize and classify EEG signals where the main characteristic can be both, rhythmic in nature as in motor imagery, and also transient in time space, like the P300 has been presented.

Although single trial classification was not perfectly achieved, it has been shown that this method could be applied with a P300 Speller Matrix application with increased ITR.

The adaptive behaviour of the algorithm make it well suited when the shape of the pattern elicited by the P300 response, does not conform to the predicted structure. This is due to the fact that the descriptors are directly based on how the signals actually looked like for the training and calibration step, and they do not require any prior knowledge about the signal. This is of particular relevance for studies on outliers populations as may be the case for people who suffered some form of neuro-degenerative disorder like Lou Gehrig's disease.

The expanding of the understanding of this tool in order to automatically classify patterns in EEG, that are specifically identified by their shapes, is a prospect future work to be considered. It may also provide assistance to physician or electroencephalographers to help them locate these EEG patterns particularly in long recording periods [16], frequent in sleep research.

Moreover, this method can be used as an alternate *BCI predictor* [8] or as a tool for artefact removal (which is performed on many occasions by visually inspecting the signal).

**Acknowledgments:** This project was supported by the ITBACyT-15 funding program issued by ITBA University.

**Author Contributions:** This projects is part of a the first author's PhD Thesis which is directed by Juan Miguel Santos and codirected by Ana Julia Villar.

**Conflicts of Interest:** The authors declare no conflict of interest.

## Abbreviations

The following abbreviations are used in this manuscript:

EEG: electroencephalography

BCI: Brain Computer Interfaces

SNR: Signal to Noise Ratio

CNS: Central Nervous System

ALS: Amyotrophic Lateral Sclerosis

ERP: Event-Related Potential

P300: Positive deflection of an Event-Related Potential which occurs 300 ms after onset of stimulus

ITR: Information Transfer Rate

BTR: Bit Transfer Rate

SIFT: Scale Invariant Feature Transform

HOG: Histogram Of Gradients

## Bibliography

- Schomer, D.L.; Silva, F.L.D. *Niedermeyer's Electroencephalography: Basic Principles, Clinical Applications, and Related Fields*; Vol. 1, 2010; p. 1296.
- De Vos, M.; Debener, S. Mobile eeg: Towards brain activity monitoring during natural action and cognition. *International Journal of Psychophysiology* **2014**, *91*, 1–2.
- Wolpaw, Jonathan R, W.E. *Brain-Computer Interfaces: Principles and Practice*; Oxford University Press, 2012; p. 400.
- Carlson, T.; del R. Millan, J. Brain-Controlled Wheelchairs: A Robotic Architecture. *IEEE Robotics & Automation Magazine* **2013**, *20*, 65–73.
- Guger, C.; Daban, S.; Sellers, E.; Holzner, C.; Krausz, G.; Carabalona, R.; Gramatica, F.; Edlinger, G. How many people are able to control a P300-based brain-computer interface (BCI)? *Neuroscience Letters* **2009**, *462*, 94–98.
- Jure, F.A.; Carrere, L.C.; Gentiletti, G.G.; Tabernig, C.B. BCI-FES system for neuro-rehabilitation of stroke patients. *Journal of Physics: Conference Series* **2016**, *705*, 012058.
- Chen, G. Are electroencephalogram (EEG) signals pseudo-random number generators? *Journal of Computational and Applied Mathematics* **2014**, *268*, 1–4.
- Clerc, M.; Bougrain, L.; Lotte, F. *Brain-computer interfaces. 2, Technology and applications*; p. 331.



9. Nijboer, F.; Broermann, U. Brain–Computer Interfaces for Communication and Control in Locked-in Patients; Springer Berlin Heidelberg, 2009; pp. 185–201.
10. Riener, R.; Seward, L.J. Cybathlon 2016. *2014 IEEE International Conference on Systems, Man, and Cybernetics (SMC)* **2014**, pp. 2792–2794.
11. Huggins, J.E.; Alcaide-Aguirre, R.E.; Hill, K. Effects of text generation on P300 brain-computer interface performance. *Brain-Computer Interfaces* **2016**, *3*, 112–120.
12. Ramele, R.; Villar, A.J.; Santos, J.M. BCI classification based on signal plots and SIFT descriptors. 4th International Winter Conference on Brain-Computer Interface, BCI 2016; IEEE: Yongpyong, 2016; pp. 1–4.
13. Knuth, K.H.; Shah, A.S.; Truccolo, W.A.; Ding, M.; Bressler, S.L.; Schroeder, C.E. Differentially Variable Component Analysis: Identifying Multiple Evoked Components Using Trial-to-Trial Variability. *Journal of Neurophysiology* **2006**, *95*.
14. Alvarado-González, M.; Garduño, E.; Bribiesca, E.; Yáñez-Suárez, O.; Medina-Bañuelos, V.; Bribiesca, E. P300 Detection Based on EEG Shape Features. *Computational and Mathematical Methods in Medicine* **2016**, *2016*, 1–14.
15. Yamaguchi, T.; Fujio, M.; Inoue, K.; Pfurtscheller, G. Design Method of Morphological Structural Function for Pattern Recognition of EEG Signals During Motor Imagery and Cognition. 2009 Fourth International Conference on Innovative Computing, Information and Control (ICICIC). IEEE, 2009, pp. 1558–1561.
16. Hartman, a.L. *Atlas of EEG Patterns*; Vol. 65, 2005; pp. E6–E6.
17. Riccio, A.; Simone, L.; Schettini, F.; Pizzimenti, A.; Inghilleri, M.; Belardinelli, M.O.; Mattia, D.; Cincotti, F. Attention and P300-based BCI performance in people with amyotrophic lateral sclerosis. *Frontiers in Human Neuroscience* **2013**, *7*, 732.
18. Brunner, C.; Blankertz, B.; Cincotti, F.; Kübler, A.; Mattia, D.; Miralles, F.; Nijholt, A.; Otal, B. BNCI Horizon 2020 – Towards a Roadmap for Brain / Neural Computer Interaction. *Lecture Notes in Computer Science* **2014**, *8513*, 475–486.
19. Vedaldi, A.; Fulkerson, B. VLFeat - An open and portable library of computer vision algorithms. *Design* **2010**, *3*, 1–4.
20. Liang, N.; Bougrain, L. Averaging techniques for single-trial analysis of oddball event-related potentials. *4th International Brain-Computer ...* **2008**, pp. 1–6.
21. Lowe, G. SIFT - The Scale Invariant Feature Transform. *International Journal* **2004**, *2*, 91–110.
22. Boiman, O.; Shechtman, E.; Irani, M. In defense of nearest-neighbor based image classification. *26th IEEE Conference on Computer Vision and Pattern Recognition, CVPR* **2008**.
23. Tibon, R.; Levy, D.A. Striking a balance: analyzing unbalanced event-related potential data. *Frontiers in psychology* **2015**, *6*, 555.